AIP Journal of Applied Physics

Semi-analytical solution to the frequency-dependent Boltzmann transport equation for cross-plane heat conduction in thin films

Chengyun Hua and Austin J. Minnich

Citation: Journal of Applied Physics **117**, 175306 (2015); doi: 10.1063/1.4919432
View online: http://dx.doi.org/10.1063/1.4919432
View Table of Contents: http://scitation.aip.org/content/aip/journal/jap/117/17?ver=pdfcov
Published by the AIP Publishing

JOURNAL OF APPLIED PHYSICS **117**, 175306 (2015)

Semi-analytical solution to the frequency-dependent Boltzmann transport equation for cross-plane heat conduction in thin films

Chengyun Hua and Austin J. Minnich[a)]
Division of Engineering and Applied Science, California Institute of Technology, Pasadena, California 91125, USA

(Received 4 March 2015; accepted 18 April 2015; published online 5 May 2015)

Cross-plane heat transport in thin films with thicknesses comparable to the phonon mean free paths is of both fundamental and practical interest for applications such as light-emitting diodes and quantum well lasers. However, physical insight is difficult to obtain for the cross-plane geometry due to the challenge of solving the Boltzmann equation in a finite domain. Here, we present a semi-analytical series expansion method to solve the transient, frequency-dependent Boltzmann transport equation that is valid from the diffusive to ballistic transport regimes and rigorously includes the frequency-dependence of phonon properties. Further, our method is more than three orders of magnitude faster than prior numerical methods and provides a simple analytical expression for the thermal conductivity as a function of film thickness. Our result enables a straightforward physical understanding of cross-plane heat conduction in thin films. © *2015 AIP Publishing LLC*. [http://dx.doi.org/10.1063/1.4919432]

I. INTRODUCTION

In the past two decades, thermal transport in thin solid films with thicknesses from tens of nanometers to micrometers has become a topic of considerable importance.[1–4] Such films are used in applications ranging from quantum well lasers to electronic devices.[5–7] For example, boundary scattering in these films leads to reduced thermal conductivity that results in the inefficient removal of heat in GaN transistors and light emitting diodes (LEDs).[8–10] To address these and other problems, it is first necessary to understand the fundamental physics of heat conduction in micro-scale solid thin films.

Heat transport in thin films with thicknesses comparable to the phonon mean free paths (MFPs) is governed by the Boltzmann transport equation (BTE), which is an integro-differential equation of time, real space, and phase space. Due to its high dimensionality, it is in general very challenging to solve. For transport along the thin film, an analytical solution can be easily derived by assuming that the characteristic length scale of the thermal gradient is much longer than the phonon MFPs. Analytical solutions were derived for electron transport by Fuchs and Sondheimer with partially specular and partially diffuse boundary scattering.[11,12] Later, the Fuchs-Sondheimer solutions were extended to phonon thermal transport assuming an average phonon MFP, enabling the calculation of thermal conductivity as a function of the film thickness.[13,14] Mazumder and Majumdar used a Monte-Carlo method to study the phonon transport along a silicon thin film including phonon dispersion and polarizations.[15]

Heat conduction perpendicular to the thin film (cross-plane direction) is much more challenging. In other fields such as neutron transport and thermal radiation, solutions to the BTE for a slab geometry have been obtained using an invariant embedding method,[16,17] an iterative method,[18] and an eigenfunction expansion approach.[19] For heat conduction, Majumdar numerically solved the gray phonon Boltzmann transport using a discrete-ordinate method by assuming that the two surfaces of the film were black phonon emitters.[20] Later, Joshi and Majumdar developed an equation of phonon radiative transfer for both steady-state and transient cases, which showed the correct limiting behavior for both purely ballistic and diffusive transport.[21] Chen and Tien applied solutions from radiative heat transfer to calculate the thermal conductivity of a thin film attached to two thermal reservoirs.[13] Chen obtained approximate analytical solutions of the BTE to study ballistic phonon transport in the cross-plane direction of superlattices and addressed the inconsistent use of temperature definition at the interfaces.[22] Cross-plane heat conduction using a consistent temperature definition was then re-investigated by Chen and Zeng.[23,24]

Despite these extensive efforts to study transport in thin films based on the BTE, solutions for the cross-plane geometry are still only available with expensive numerical calculations. For example, no analogous Fuchs-Sondheimer formula for the in-plane thermal conductivity exists for the cross-plane direction. Furthermore, most of the previous approaches assumed a single phonon MFP even though recent work has demonstrated that the transport properties of phonons in solids vary widely over the broad thermal spectrum.[25,26] Incorporating frequency-dependent phonon properties with these prior numerical methods is extremely computationally expensive.

In this work, we present a semi-analytical solution of the frequency-dependent transient BTE using the method of degenerate kernels, also known as a series expansion method.[27] Our approach is valid from the diffusive to ballistic transport regimes, is capable of incorporating a variety of boundary conditions, and is more than three orders of

[a)]aminnich@caltech.edu

magnitude faster than prior numerical approaches. Further, we obtain a simple closed-form expression for cross-plane thermal conductivity, analogous to the Fuch-Sondheimer formula for the in-plane thermal conductivity, which enables the cross-plane thermal conductivity of a thin film to be easily calculated. Our results can be applied to efficiently solve heat conduction problems in numerous practical geometries such as superlattices and the thin films used in thermoreflectance experiments while rigorously incorporating the full phonon dispersion.

II. THEORY

A. Governing equation

The one-dimensional (1D) frequency-dependent BTE for an isotropic crystal under the relaxation time approximation is given by

$$\frac{\partial g_\omega}{\partial t} + v_g \mu \frac{\partial g_\omega}{\partial x} = -\frac{g_\omega - g_0(T)}{\tau_\omega} + \frac{Q_\omega}{4\pi}, \tag{1}$$

where $g_\omega = \hbar\omega(f_\omega(x,t,\theta) - f_0(T_0))$ is the desired deviational energy distribution function, $g_0(T)$ is the equilibrium deviational distribution function defined below, Q_ω is the spectral volumetric heat generation, v_g is the phonon group velocity, and τ_ω is the phonon relaxation time. Here, x is the spatial variable, t is the time, ω is the phonon frequency, T is the temperature, and $\mu = \cos(\theta)$ is the directional cosine of the polar angle.

Assuming a small temperature rise, $\Delta T = T - T_0$, relative to a reference temperature, T_0, the equilibrium deviational distribution is proportional to ΔT

$$g_0(T) = \frac{1}{4\pi}\hbar\omega D(\omega)\left(f_{BE}(T) - f_{BE}(T_0)\right) \approx \frac{1}{4\pi} C_\omega \Delta T. \tag{2}$$

Here, $\hbar$ is the reduced Planck constant, $D(\omega)$ is the phonon density of states, f_{BE} is the Bose-Einstein distribution, and $C_\omega = \hbar\omega D(\omega)\frac{\partial f_{BE}}{\partial T}$ is the mode specific heat. The volumetric heat capacity is then given by $C = \int_0^{\omega_m} C_\omega d\omega$ and the thermal conductivity $k = \int_0^{\omega_m} k_\omega d\omega$, where $k_\omega = \frac{1}{3} C_\omega v_\omega \Lambda_\omega$ and $\Lambda_\omega = \tau_\omega v_\omega$ is the phonon MFP.

Both g_ω and ΔT are unknown. Therefore, to close the problem, energy conservation is used to relate g_ω to ΔT, given by

$$\int\int_0^{\omega_m} \left[\frac{g_\omega(x,t)}{\tau_\omega} - \frac{1}{4\pi}\frac{C_\omega}{\tau_\omega}\Delta T(x,t)\right] d\omega d\Omega = 0, \tag{3}$$

where Ω is the solid angle in spherical coordinates and ω_m is the cut-off frequency. Note that summation over phonon branches is implied without an explicit summation sign whenever an integration over phonon frequency is performed.

To solve this equation, we first transform it into an inhomogeneous first-order differential equation by applying a Fourier transform to the time variable, giving

$$i\eta\tilde{g}_\omega + v_g\mu\frac{d\tilde{g}_\omega}{dx} = -\frac{\tilde{g}_\omega}{\tau_\omega} + \frac{C_\omega}{\tau_\omega}\frac{\Delta\tilde{T}}{4\pi} + \frac{\tilde{Q}_\omega}{4\pi}, \tag{4}$$

where η is the temporal frequency. This equation has the general solution

$$\tilde{g}_\omega^+(x) = P_\omega e^{-\frac{\gamma_\omega}{\mu}x} + \int_0^x \frac{C_\omega\Delta\tilde{T}(x') + \tilde{Q}_\omega(x')\tau_\omega}{4\pi\Lambda_\omega\mu} \times e^{\frac{\gamma_\omega}{\mu}(x'-x)}dx' \ (\mu \in (0,1]), \tag{5}$$

$$\tilde{g}_\omega^-(x) = B_\omega e^{\frac{\gamma_\omega}{\mu}(L-x)} - \int_x^L \frac{C_\omega\Delta\tilde{T}(x') + \tilde{Q}_\omega(x')\tau_\omega}{4\pi\Lambda_\omega\mu} \times e^{\frac{\gamma_\omega}{\mu}(x'-x)}dx' \ (\mu \in [-1,0]), \tag{6}$$

where $\gamma_\omega = (1 + i\eta\tau_\omega)/\Lambda_\omega$, L is the distance between the two walls, and P_ω and B_ω are the unknown coefficients determined by the boundary conditions. Here, $\tilde{g}^+(x)$ indicates the forward-going phonons and $\tilde{g}^-(x)$ the backward-going phonons. In this work, $\tilde{g}^+(x)$ is specified at one of the two walls and $\tilde{g}^-(x)$ is specified at the other.

Let us assume that the two boundaries are nonblack but diffuse with wall temperature ΔT_1 and ΔT_2, respectively. The boundary conditions can be written as

$$\tilde{g}_\omega^+(x=0) = P_\omega = \epsilon_1\frac{C_\omega}{4\pi}\Delta T_1 + (1-\epsilon_1)\int_{-1}^0 \tilde{g}_\omega^-(x=0,\mu)d\mu, \tag{7}$$

$$\tilde{g}_\omega^-(x=L) = B_\omega = \epsilon_2\frac{C_\omega}{4\pi}\Delta T_2 + (1-\epsilon_2)\int_0^1 \tilde{g}_\omega^+(x=L,\mu)d\mu, \tag{8}$$

where ϵ_1 and ϵ_2 are the emissivities of the hot and cold walls, respectively. When $\epsilon_1 = \epsilon_2 = 1$, the walls are black and we recover Dirichlet boundary conditions. Note that while we assume a thermal spectral distribution for the boundary condition, an arbitrary spectral profile can be specified by replacing the thermal distribution with the desired distribution. Equations (7) and (8) are specific for diffuse boundary scattering; the specular case is presented in Appendix A.

Applying the boundary conditions to Eqs. (5) and (6), we have

$$\tilde{g}_\omega^+(x) = A_{1\omega}\frac{C_\omega}{4\pi}e^{-\frac{\gamma_\omega}{\mu}x} + e^{-\frac{\gamma_\omega}{\mu}x}\int_0^L \frac{C_\omega\Delta\tilde{T}(x') + \tilde{Q}_\omega(x')\tau_\omega}{4\pi\Lambda_\omega} \times \left[D_\omega E_1\left(\gamma_\omega(L-x')\right) + B_{1\omega}E_1\left(\gamma_\omega x'\right)\right]dx' + \int_0^x \frac{C_\omega\Delta\tilde{T}(x') + \tilde{Q}_\omega(x')\tau_\omega}{4\pi\Lambda_\omega\mu}e^{\frac{\gamma_\omega}{\mu}(x'-x)}dx' \ (\mu \in [0,1]), \tag{9}$$

$$\tilde{g}_\omega^-(x) = A_{2\omega}\frac{C_\omega}{4\pi}e^{-\frac{\gamma_\omega}{\mu}(L-x)} + e^{-\frac{\gamma_\omega}{\mu}(L-x)}\int_0^L \frac{C_\omega\Delta\tilde{T}(x') + \tilde{Q}_\omega(x')\tau_\omega}{4\pi\Lambda_\omega} \times \left[D_\omega E_1\left(\gamma_\omega x'\right) + B_{2\omega}E_1\left(\gamma_\omega(L-x')\right)\right]dx' + \int_x^L \frac{C_\omega\Delta\tilde{T}(x') + \tilde{Q}_\omega(x')\tau_\omega}{4\pi\Lambda_\omega\mu}e^{-\frac{\gamma_\omega}{\mu}(x'-x)}dx' \ (\mu \in [0,1]), \tag{10}$$

where

$$A_{1\omega} = \frac{\epsilon_1 \Delta T_1 + (1-\epsilon_1)\epsilon_2 \Delta T_2 E_2(\gamma_\omega L)}{1-(1-\epsilon_1)(1-\epsilon_2)(E_2(\gamma_\omega L))^2},$$

$$A_{2\omega} = \frac{\epsilon_2 \Delta T_2 + (1-\epsilon_2)\epsilon_1 \Delta T_1 E_2(\gamma_\omega L)}{1-(1-\epsilon_1)(1-\epsilon_2)(E_2(\gamma_\omega L))^2},$$

$$B_{1\omega} = \frac{1-\epsilon_1}{1-(1-\epsilon_1)(1-\epsilon_2)(E_2(\gamma_\omega L))^2},$$

$$B_{2\omega} = \frac{1-\epsilon_2}{1-(1-\epsilon_1)(1-\epsilon_2)(E_2(\gamma_\omega L))^2},$$

$$D_\omega = \frac{(1-\epsilon_1)(1-\epsilon_2)E_2(\gamma_\omega L)}{1-(1-\epsilon_1)(1-\epsilon_2)(E_2(\gamma_\omega L))^2},$$

and $E_n(x)$ is the exponential integral given by[28]

$$E_n(x) = \int_0^1 \mu^{n-2} e^{-\frac{x}{\mu}} d\mu. \tag{11}$$

To close the problem, we plug Eqs. (9) and (10) into Eq. (3) and obtain an integral equation for temperature as

$$\begin{aligned} 2\int_0^{\omega_m} \frac{C_\omega}{\tau_\omega} d\omega \Delta\tilde{T}(\hat{x}) &= \int_0^{\omega_m} \frac{C_\omega}{\tau_\omega} \left[A_{1\omega} E_2(\hat{\gamma}_\omega \hat{x}) + A_{2\omega} E_2\left(\hat{\gamma}_\omega (1-\hat{x})\right)\right] d\omega \\ &+ \int_0^1 \int_0^{\omega_m} \tilde{Q}_\omega(x') \frac{G_\omega(\hat{x},\hat{x}')}{\mathrm{Kn}_\omega} d\omega d\hat{x}' \\ &+ \int_0^1 \Delta\tilde{T}(\hat{x}') \int_0^{\omega_m} \frac{C_\omega G_\omega(\hat{x},\hat{x}')}{\mathrm{Kn}_\omega \tau_\omega} d\omega d\hat{x}', \end{aligned} \tag{12}$$

where $\hat{x} = x/L$, $\mathrm{Kn}_\omega = \Lambda_\omega/L$ is the Knudsen number, $\hat{\gamma}_\omega = \frac{1+i\eta\tau_\omega}{\mathrm{Kn}_\omega}$ and

$$\begin{aligned} G_\omega(\hat{x},\hat{x}') = &E_2(\hat{\gamma}_\omega \hat{x})[D_\omega E_1(\hat{\gamma}_\omega(1-\hat{x}')) + B_{1\omega} E_1(\hat{\gamma}_\omega \hat{x}')] \\ &+ E_2(\hat{\gamma}_\omega(1-\hat{x}))[D_\omega E_1(\hat{\gamma}_\omega \hat{x}') \\ &+ B_{1\omega} E_1(\hat{\gamma}_\omega(1-\hat{x}'))] + E_1(\hat{\gamma}_\omega|\hat{x}'-\hat{x}|). \end{aligned} \tag{13}$$

Equation (12) can be written in the form

$$\Delta T(\hat{x}) = f(\hat{x}) + \int_0^1 K(\hat{x},\hat{x}') \Delta T(\hat{x}') d\hat{x}', \tag{14}$$

where the kernel function $K(\hat{x},\hat{x}')$ is given by

$$K(\hat{x},\hat{x}') = \frac{1}{2\int_0^{\omega_m} \frac{C_\omega}{\tau_\omega} d\omega} \int_0^{\omega_m} \frac{C_\omega G_\omega(\hat{x},\hat{x}')}{\mathrm{Kn}_\omega \tau_\omega} d\omega \tag{15}$$

and the inhomogeneous function $f(\hat{x})$ is given by

$$\begin{aligned} f(\hat{x}) = &\frac{1}{2\int_0^{\omega_m} \frac{C_\omega}{\tau_\omega} d\omega} \int_0^{\omega_m} \frac{C_\omega}{\tau_\omega} \\ &\times \left[A_{1\omega} E_2(\hat{\gamma}_\omega \hat{x}) + A_{2\omega} E_2\left(\hat{\gamma}_\omega(1-\hat{x})\right)\right] d\omega \\ &+ \frac{1}{2\int_0^{\omega_m} \frac{C_\omega}{\tau_\omega} d\omega} \int_0^1 \int_0^{\omega_m} \tilde{Q}_\omega(x') \frac{G_\omega(\hat{x},\hat{x}')}{\mathrm{Kn}_\omega} d\omega d\hat{x}'. \end{aligned} \tag{16}$$

From Eq. (14), we see that the governing equation is a Fredholm integral equation of the second kind. Previously, the gray version of Eq. (12) that assumes average phonon properties has been solved numerically using integral discretization method.[28] While this approach does yield the solution, it requires the filling and inversion of a large, dense matrix, an expensive calculation even for the gray case. Considering the full phonon dispersion adds additional integrations to calculate each element of the matrix, dramatically increasing the computational cost. Additionally, care must be taken to account for a singularity point at $\hat{x}' = \hat{x}$ since $E_1(0) \to \infty$.

B. Method of degenerate kernels

Here, we solve this equation using the method of degenerate kernels,[27] which is much more efficient than the integral discretization method and automatically accounts for the singularity point at $\hat{x}' = \hat{x}$. This method is based on expanding all the functions in Eq. (14) in a Fourier series, then solving for the coefficients of the temperature profile. From the temperature $\Delta\tilde{T}(\hat{x})$, all other quantities such as the distribution and heat flux can be obtained.

To apply this method, we first need to expand the inhomogeneous function $f(\hat{x})$ and kernel $K(\hat{x},\hat{x}')$ with a Fourier series. This expansion is possible because both $f(\hat{x})$ and $K(\hat{x},\hat{x}')$ are continuous and continuously differentiable on the relevant spatial domains of normalized length between $[0,1]$ and $[0,1]\times[0,1]$, respectively.[27] All the necessary functions can be expanded using a linear combination of sines and cosines; however, a substantial simplification can be obtained by solving a symmetric problem in which the spatial domain is extended to include its mirror image by extending both $f(\hat{x})$ and $K(\hat{x},\hat{x}')$ to $[-1,1]$ and $[-1,1]\times[-1,1]$. Because of the symmetry of this domain, all the coefficients for sine functions equal zero and the Fourier series for both functions reduces to a cosine expansion. $f(\hat{x})$ is then approximated as

$$f_{(N)}(\hat{x}) = \frac{1}{2} f_0 + \sum_{m=1}^{N} f_m \cos(m\pi\hat{x}), \tag{17}$$

where $f_m = 2\int_0^1 f(\hat{x})\cos(m\pi\hat{x})d\hat{x}$. The kernel $K(\hat{x},\hat{x}')$ can be represented by a degenerate double Fourier series, given by

$$\begin{aligned} K_{(N)}(\hat{x},\hat{x}') = &\frac{1}{4}k_{00} + \frac{1}{2}\sum_{m=1}^{N} k_{m0}\cos(m\pi\hat{x}) + \frac{1}{2}\sum_{n=1}^{N} k_{0n}\cos(n\pi\hat{x}') \\ &+ \sum_{m=1}^{N}\sum_{n=1}^{N} k_{mn}\cos(m\pi\hat{x})\cos(n\pi\hat{x}'), \end{aligned} \tag{18}$$

where

$$k_{mn} = 4\int_0^1 \int_0^1 K(\hat{x},\hat{x}')\cos(m\pi\hat{x})\cos(n\pi\hat{x}')d\hat{x}d\hat{x}'. \tag{19}$$

Moreover, the convergence and completeness theorem of cosine functions guarantees that $K_{(N)}(\hat{x},\hat{x}')$ and $f_{(N)}(\hat{x})$ converge to $K(\hat{x},\hat{x}')$ and $f(\hat{x})$ as $N \to \infty$.[29]

Inserting Eqs. (17) and (18) into Eq. (14), we then obtain the following integral equation

$$\sum_{m=0}^{N} x_m \cos(m\pi\hat{x}) = \frac{1}{2}f_0 + \sum_{m=0}^{N} f_m \cos(m\pi\hat{x}) + \int_0^1 \sum_{n=0}^{N} x_m \cos(n\pi\hat{x}') \times \left[\frac{1}{4}k_{00} + \frac{1}{2}\sum_{m=1}^{N} k_{m0}\cos(m\pi\hat{x}) + \frac{1}{2}\sum_{n=1}^{N} k_{0n}\cos(n\pi\hat{x}') + \sum_{m=1}^{N}\sum_{n=1}^{N} k_{mn}\cos(m\pi\hat{x})\cos(n\pi\hat{x}')\right] d\hat{x}', \quad (20)$$

where x_m are the desired but unknown Fourier coefficients of $\Delta\tilde{T}(\hat{x})$.

Using the orthogonality of cos $(n\pi\hat{x})$ on $[0,1]$ gives a simpler form of Eq. (20)

$$\sum_{m=0}^{N} x_m \cos(m\pi\hat{x}) = \frac{1}{2}f_0 + \sum_{m=0}^{N} f_m \cos(m\pi\hat{x}) + \frac{1}{4}\sum_{m=0}^{N} k_{m0}x_m + \frac{1}{2}\sum_{m=1}^{N}\sum_{n=1}^{N} k_{mn}x_n \cos(m\pi\hat{x}). \quad (21)$$

Grouping the terms with the same index m in cosine, a system of linear equations of x_m can be obtained as

$$\bar{\bar{A}}\bar{x} = \bar{f}, \quad (22)$$

where $\bar{x}$ is the vector of unknown coefficient x_m and $\bar{f}$ is the vector of f_m in Eq. (17). The matrix $\bar{\bar{A}}$ contains elements $A_{00} = 1 - \frac{k_{00}}{4}$, $A_{0n} = -\frac{1}{2}k_{0n}$, $A_{n0} = -\frac{k_{n0}}{4}$, $A_{nn} = 1 - \frac{1}{2}k_{nn}$, and $A_{nm} = -\frac{1}{2}k_{nm}$ $(m \neq n \neq 0)$. Expressions of the elements in $\bar{\bar{A}}$ can be obtained analytically for the specific kernel here and are given in Appendix B for steady-state heat conduction with diffuse walls. Since there is no row or column in $\bar{\bar{A}}$ that is all zeros or a constant multiple of another row or column, it is always guaranteed that $\bar{\bar{A}}$ is non-singular and its inverse exists.

Solving the matrix system yields x_m and thus the temperature $\Delta\tilde{T}(\hat{x})$, $\tilde{g}_\omega^+(x)$, and $\tilde{g}_\omega^-(x)$ can be obtained from $\Delta\tilde{T}(\hat{x})$ using Eqs. (9) and (10). Finally, the spectral heat is given by

$$q_\omega(x) = \int_{-1}^{1} g_\omega v_\omega \mu d\mu = \int_0^1 g_\omega^+ v_\omega \mu d\mu - \int_0^1 g_\omega^- v_\omega \mu d\mu, \quad (23)$$

thereby closing the problem.

C. Summary of the method

We now summarize the key steps to implement our method. The first step is to determine the appropriate boundary conditions for the problem and compute the constants in Eqs. (5) and (6). Subsequently, the kernel function $K(\hat{x},\hat{x}')$ and the inhomogenous function $f(\hat{x})$ can be obtained from Eq. (3), and their Fourier coefficients can be computed using Eqs. (17) and (18). The elements in $\bar{\bar{A}}$ correspond to the Fourier coefficients of kernel function $K(\hat{x},\hat{x}')$, and $\bar{f}$ is a vector of the Fourier coefficients of the inhomogeneous part of Eq. (12). We emphasize that analytic expressions for all of these elements exist and can be obtained; examples of these coefficients for steady heat conduction with non-black, diffuse boundaries are given in Appendix B. Once $\bar{\bar{A}}$ and $\bar{f}$ are obtained, Eq. (22) is solved by standard matrix methods to yield the coefficients x_m. Finally, $\Delta\tilde{T}(\hat{x})$ is given by $\sum_{m=0}^{N} x_m \cos(m\pi\hat{x})$.

D. Efficiency of the method

The primary benefit of our method is the substantial reduction in computational cost compared to the widely used integral discretization approach. Since both $K_{(N)}(\hat{x},\hat{x}')$ and $f_{(N)}(\hat{x})$ converge to $K(\hat{x},\hat{x}')$ and $f(\hat{x})$ as $1/N^2$, only a few terms of expansion are required for accurate calculations. In practice, we find that only 20 terms are necessary before the calculation converges, meaning the required matrix is only 20×20. Compared to the traditional integral discretization method that requires a matrix on the order of 1000×1000 before convergence is achieved, our approach is at least 3 orders of magnitude faster. Further, as we will show in Sec. III, our semi-analytical approach enables a closed-form solution for the cross-plane thermal conductivity of a thin film that is not possible to derive from the integral discretization method.

E. Demonstration of the method

As an example calculation, we consider steady-state heat conduction between two walls that are either black or non-black. In the former case, both wall emissivities ϵ_1 and ϵ_2 equal 1 while in the latter case they are set to 0.5. Assuming steady state and no heat generation inside the domain, $\eta = 0$, and $Q_\omega = 0$. The Fourier coefficients of $K(\hat{x},\hat{x}')$ and $\bar{f}$ for these two specific cases are given in Appendix B. We perform our calculations for crystalline silicon, using the experimental dispersion in the [100] direction and assuming the crystals are isotropic. The numerical details concerning the dispersion and relaxation times are given in Ref. 30.

We calculate the deviational temperature distribution $\Delta T(\hat{x})$ for different film thickness at different equilibrium temperatures as shown in Fig. 1 while keeping $|\Delta T1| = |\Delta T_2| = 1$ K. When the averaged Knudsen number is small such that $\mathrm{Kn}_{avg} \ll 1$, the temperature profile remains linear. As thin film thickness decreases such that $\mathrm{Kn}_{avg} \sim 1$ or $\gg 1$, we observe a similar temperature slip as discussed in Ref. 25. These calculations take approximately one second to compute on a standard laptop computer. In contrast, the integral discretization method is at least 1000 times slower, requiring on the order of one hour to arrive at the same result.

In addition to the finite-layer geometry we consider above, the series expansion approach can be readily applied to many other thin film geometries, such as superlattices and the transducer film used in thermoreflectance experiments, by imposing different boundary conditions. Similar large

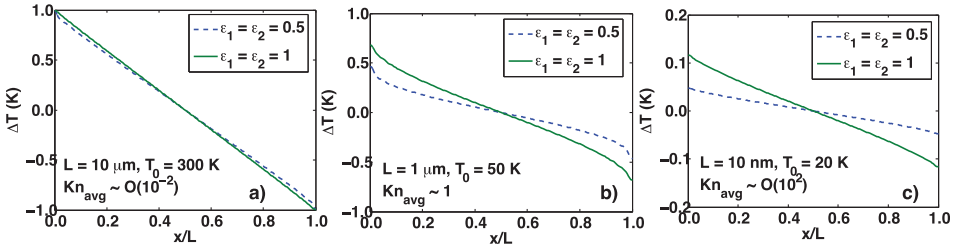

FIG. 1. Temperature distribution $\Delta T(\hat{x})$ for a planar slab with black walls (solid lines) and nonblack walls (dashed lines) when (a) $\mathrm{Kn}_{\mathrm{avg}} \sim O(10^{-2})$, (b) $\mathrm{Kn}_{\mathrm{avg}} \sim 1$, and (c) $\mathrm{Kn}_{\mathrm{avg}} \sim O(10^{2})$. As $\mathrm{Kn}_{\mathrm{avg}}$ increases, temperature slip at the boundaries grows larger.

reductions in computational cost can be expected for these cases.

III. ANALYTICAL FORMULA FOR CROSS-PLANE THERMAL CONDUCTIVITY

Our semi-analytical approach also allows us to obtain a simple closed form expression for the cross-plane thermal conductivity as a function of film thickness, analogous to the Fuchs-Sondheimer expression for in-plane thermal conductivity. Such a formula allows the cross-plane thermal conductivity to be easily evaluated because the full solution of the BTE is no longer required. To derive this formula, we assume black walls and calculate the spatially averaged spectral heat flux that is integrated over the domain, defined as

$$\begin{aligned}\int_0^1 q_\omega(\hat{x})d\hat{x} &= \frac{1}{L}\int_0^L q_\omega(x)dx \\ &= \left(\frac{\Delta T_1 - \Delta T_2}{2}\right)\left[\frac{1}{3}C_\omega v_\omega \mathrm{Kn}_\omega \right. \\ &\quad \left. - C_\omega v_\omega \mathrm{Kn}_\omega E_4\left(\frac{1}{\mathrm{Kn}_\omega}\right)\right] \\ &\quad + \frac{C_\omega v_\omega}{2\mathrm{Kn}_\omega}\left[\int_0^1\int_0^{\hat{x}} \Delta T(\hat{x}')E_2\left(\frac{|\hat{x}'-\hat{x}|}{\mathrm{Kn}_\omega}\right)d\hat{x}'d\hat{x}\right. \\ &\quad \left. - \int_0^1\int_{\hat{x}}^1 \Delta T(\hat{x}')E_2\left(\frac{|\hat{x}'-\hat{x}|}{\mathrm{Kn}_\omega}\right)d\hat{x}'d\hat{x}\right]. \end{aligned} \tag{24}$$

Once x_m is solved from Eq. (20), we can insert the Fourier series of $\Delta T(x)$ into Eq. (24), which leads to

$$\begin{aligned}&\int_0^1 q_\omega(\hat{x})d\hat{x} \\ &= \left[\left(\frac{\Delta T_1 - \Delta T_2}{2}\right)\frac{1}{3}C_\omega v_\omega \mathrm{Kn}_\omega - C_\omega v_\omega \mathrm{Kn}_\omega E_4\left(\frac{1}{\mathrm{Kn}_\omega}\right)\right] \\ &\quad + \frac{C_\omega v_\omega}{2\mathrm{Kn}_\omega}\sum_{m=1}^{\infty} x_m\left[1-(-1)^m\right]\int_0^1 \frac{(\mathrm{Kn}_\omega\mu)^2\left(1+e^{-\frac{1}{\mathrm{Kn}_\omega\mu}}\right)}{1+(\mathrm{Kn}_\omega\mu)^2(m\pi)^2}d\mu. \end{aligned} \tag{25}$$

According to Fourier's law, the integrated heat flux is given by

$$\int_0^1 q_\omega^f(\hat{x})d\hat{x} = \frac{1}{3}C_\omega v_\omega \mathrm{Kn}_\omega(\Delta T_1 - \Delta T_2). \tag{26}$$

The heat suppression function is defined as the ratio of the BTE and Fourier's heat flux,[31] given as

$$\begin{aligned}S(\mathrm{Kn}_\omega, L) &= \frac{1}{2} - \frac{3}{2}E_4\left(\frac{1}{\mathrm{Kn}_\omega}\right) + \frac{3}{2}\sum_{m=1}^{\infty} x_m\left[1-(-1)^m\right] \\ &\quad \times \int_0^1 \frac{\mu^2\left(1+e^{-\frac{1}{\mathrm{Kn}_\omega\mu}}\right)}{1+(\mathrm{Kn}_\omega\mu)^2(m\pi)^2}d\mu. \end{aligned} \tag{27}$$

Note that the suppression function in general not only depends on Kn_ω but also is a function of geometry through x_m. The reduced or apparent thermal conductivity at a given domain thickness L is then given by

$$k(L) = \int_0^{\omega_m} \frac{1}{3}C_\omega v_\omega \Lambda_\omega S(\mathrm{Kn}_\omega, L)d\omega. \tag{28}$$

This formula is analogous to the Fuch-Sondheimer equation for transport along thin films and allows the evaluation of the cross-plane thermal conductivity provided the expansion coefficients x_m are known. However, obtaining the expansion coefficients still requires solving the BTE as described in Sec. II B. A more useful result would be a suppression function that depends only on the Knudsen number as is available for in-plane heat conduction with the Fuchs-Sondheimer formula.[11,12]

To overcome this difficulty, we derive a simplified form of Eq. (27) that is valid under the conditions of most experiments. Note from Fig. 1(a) that for $\mathrm{Kn}_{avg} \sim O(10^{-2})$, the temperature distribution is still linear, allowing us to simplify Eq. (27) by inserting the linear temperature distribution. Doing so leads to a simplified suppression function

$$S_{\mathrm{simplified}}(\mathrm{Kn}_\omega) = 1 + 3\mathrm{Kn}_\omega\left[E_5\left(\frac{1}{\mathrm{Kn}_\omega}\right) - \frac{1}{4}\right]. \tag{29}$$

This equation depends only on the Knudsen number and hence can be used to directly evaluate the cross-plane thermal conductivity given the phonon dispersion. This equation is valid provided that the ballistic modes are only low frequency phonons that contribute little to heat capacity, a situation that occurs often in experiment because high frequency phonons have short MFPs, on the order of tens of nanometers, at temperatures exceeding 20 K.

One important observation from Fig. 2(a) is that the exact and simplified suppression functions converge to the same curve at large Kn_ω. Also note that as the slab thickness decreases, the Knudsen number of a phonon with a particular MFP becomes larger. Therefore, in the limit of very small distance between the boundaries, the only important portion of the suppression function is at large values of Knudsen number exceeding $\mathrm{Kn}_\omega = 1$ because phonons possess a finite minimum MFP. This observation suggests that for practical

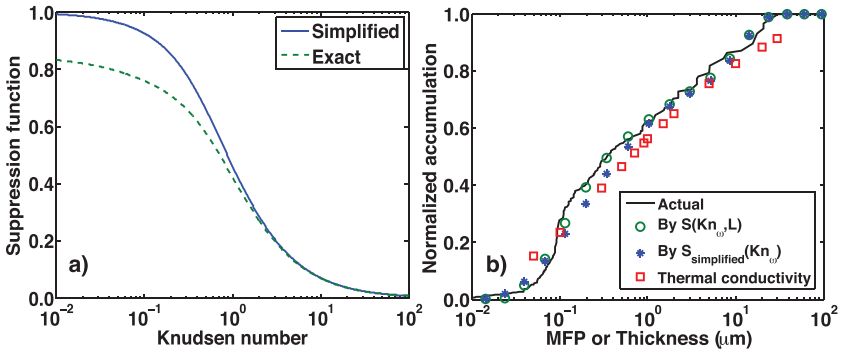

FIG. 2. (a) Simplified (solid line) and exact (dashed line) suppression function versus Knudsen number. The exact and simplified suppression functions converge to the same curve at large Kn_ω. (b) Example MFP reconstructions for silicon at 300 K using numerically simulated data. Plotted are the analytical MFP distribution (solid line), the numerical apparent thermal conductivities (squares), and the reconstructed MFP distribution by the exact suppression function (circles) and by the simplified suppression function (stars). The x axis corresponds to the MFP for the distributions and to the slab thickness for the thermal conductivity data. Both the exact and simplified suppression functions yield satisfactory MFP reconstruction results.

purposes the simplified suppression can be used even outside the range in which it is strictly valid with good accuracy. This simplification is very desirable because the simplified suppression function only depends on the Knudsen number and thus can be applied without any knowledge of other material properties.

To investigate the accuracy of this approximation, we perform a reconstruction procedure developed by Minnich[31] to recover the MFP spectrum from thermal conductivity data as a function of slab thickness using both exact and simplified suppression functions. We follow the exact procedures of the numerical method as described in Ref. 31. Briefly, we synthesize effective thermal conductivities numerically using Eq. (28). Using these effective thermal conductivities and our knowledge of the suppression function, we use convex optimization to solve for the MFP spectrum. In the exact suppression function case, each slab thickness has its own suppression function given by Eq. (27) while in the simplified case Eq. (29) is used for all slab thicknesses.

As shown in Fig. 2(b), both the simplified and exact suppression functions yield satisfactory results. Even though the smallest thickness we consider here is 50 nm, close to the ballistic regime, the simplified suppression function still gives a decent prediction over the whole MFP spectrum, with a maximum of 15% deviation from the actual MFP spectrum. For practical purposes, this deviation is comparable to uncertainties in experimental measurements and therefore the simplified suppression function can be used as an excellent approximation in the reconstruction procedure. This result demonstrates that length-dependent thermal conductivity measurements like those recently reported for SiGe nanowires[32] and graphene ribbons[33] can be used to reconstruct the full MFP spectrum rather than only an average MFP. We perform an investigation of our approach for this purpose in Ref. 34.

IV. SUMMARY

We have presented a series expansion method to solve the one-dimensional, transient frequency-dependent BTE in a finite domain and demonstrated its capability to describe cross-plane heat conduction in thin films. Our solution is valid from the diffusive to ballistic regimes with a variety of boundary conditions, rigorously includes frequency dependence, and is more than three orders of magnitude faster than prior numerical approaches. We have also developed a simple analytical expression for thermal conductivity, analogous to the Fuchs-Sondheimer equation for in-plane transport, which enables the simple calculation of the cross-plane thermal conductivity as a function of film thickness. Our work provides an efficient method to solve cross-plane heat conduction problems that occurs in numerous situations such as in superlattices and thermoreflectance experiments.

ACKNOWLEDGMENTS

This work was sponsored in part by the National Science Foundation under Grant No. CBET CAREER 1254213, and by Boeing under the Boeing-Caltech Strategic Research and Development Relationship Agreement.

APPENDIX A: SPECULAR BOUNDARIES

Here, we derive the governing equation for the problem of nonblack, specular boundaries with wall temperatures ΔT_1 and ΔT_2, respectively. The boundary conditions can be written as

$$\tilde{g}_\omega^+(x=0,\mu) = P_\omega = \epsilon_1 \frac{C_\omega}{4\pi}\Delta T_1 + (1-\epsilon_1)\tilde{g}_\omega^-(x=0,-\mu), \tag{A1}$$

$$\tilde{g}_\omega^-(x=L,\mu) = B_\omega = \epsilon_2 \frac{C_\omega}{4\pi}\Delta T_2 + (1-\epsilon_2)\tilde{g}_\omega^+(x=L,-\mu). \tag{A2}$$

Applying the boundary conditions to Eqs. (5) and (6), we have

$$\begin{aligned}\tilde{g}_\omega^+(x) =& F_1\Delta T_1 \frac{C_\omega}{4\pi} e^{-\frac{\gamma_\omega}{\mu}x} + (1-\epsilon_1)F_2\Delta T_2 \frac{C_\omega}{4\pi} e^{-\frac{\gamma_\omega}{\mu}(L+x)} \\ &+(1-\epsilon_1)F_2\int_0^L \frac{C_\omega\Delta\tilde{T}(x') + \tilde{Q}_\omega(x')\tau_\omega}{4\pi\Lambda_\omega\mu} e^{-\frac{\gamma_\omega}{\mu}(x'+x)}dx' \\ &+\int_0^x \frac{C_\omega\Delta\tilde{T}(x') + \tilde{Q}_\omega(x')\tau_\omega}{4\pi\Lambda_\omega\mu} e^{\frac{\gamma_\omega}{\mu}(x'-x)}dx' \ (\mu\in[0,1]),\end{aligned} \tag{A3}$$

$$\tilde{g}_\omega^-(x) = F_2\Delta T_2\frac{C_\omega}{4\pi}e^{-\frac{\gamma_\omega}{\mu}(L-x)} + (1-\epsilon_2)F_1\Delta T_1\frac{C_\omega}{4\pi}e^{-\frac{\gamma_\omega}{\mu}(2L-x)} + (1-\epsilon_2)F_1\int_0^L\frac{C_\omega\Delta\tilde{T}(x')+\tilde{Q}_\omega(x')\tau_\omega}{4\pi\Lambda_\omega\mu}e^{-\frac{\gamma_\omega}{\mu}(2L-x'-x)}dx' + \int_x^L\frac{C_\omega\Delta\tilde{T}(x')+\tilde{Q}_\omega(x')\tau_\omega}{4\pi\Lambda_\omega\mu}e^{-\frac{\gamma_\omega}{\mu}(x'-x)}dx' \ (\mu\in[0,1]), \tag{A4}$$

where $F_1 = \frac{\epsilon_1}{\epsilon_1+\epsilon_2-\epsilon_1\epsilon_2}$ and $F_2 = \frac{\epsilon_2}{\epsilon_1+\epsilon_2-\epsilon_1\epsilon_2}$.

To close the problem, we insert Eqs. (A3) and (A4) into Eq. (3) and nondimensionalize x by L. We then derive an integral equation for temperature for the specular boundary conditions, given by

$$2\int_0^{\omega_m}\frac{C_\omega}{\tau_\omega}d\omega\Delta\tilde{T}(\hat{x}) = \int_0^{\omega_m}\frac{C_\omega}{\tau_\omega}H_\omega(\hat{x})d\omega + \int_0^1\int_0^{\omega_m}\tilde{Q}_\omega(x')\frac{G_\omega(\hat{x},\hat{x}')}{\mathrm{Kn}_\omega}d\omega d\hat{x}' + \int_0^1\Delta\tilde{T}(\hat{x}')\int_0^{\omega_m}\frac{C_\omega G_\omega(\hat{x},\hat{x}')}{\mathrm{Kn}_\omega\tau_\omega}d\omega d\hat{x}', \tag{A5}$$

where $\hat{x} = x/L$, $\mathrm{Kn}_\omega = \Lambda_\omega/L$ is the Knudsen number, $\hat{\gamma}_\omega = \frac{1+i\eta\tau_\omega}{\mathrm{Kn}_\omega}$ and

$$H_\omega(\hat{x}) = F_1\Delta T_1E_2(\hat{\gamma}_\omega\hat{x}) + F_2\Delta T_2E_2(\hat{\gamma}_\omega(1-\hat{x})) + (1-\epsilon_1)F_2\Delta T_2E_2(\hat{\gamma}_\omega(1+\hat{x})) + (1-\epsilon_2)F_1\Delta T_1E_2(\hat{\gamma}_\omega(2-\hat{x})) \tag{A6}$$

and

$$G_\omega(\hat{x},\hat{x}') = (1-\epsilon_1)F_2E_1(\hat{\gamma}_\omega(\hat{x}+\hat{x}')) + (1-\epsilon_2)F_1E_1(\hat{\gamma}_\omega(2-\hat{x}-\hat{x}')) + E_1(\hat{\gamma}_\omega|\hat{x}-\hat{x}'|). \tag{A7}$$

In this case, the inhomogeneous function becomes

$$f(\hat{x}) = \frac{1}{2\int_0^{\omega_m}\frac{C_\omega}{\tau_\omega}d\omega}\left[\int_0^{\omega_m}\frac{C_\omega}{\tau_\omega}H_\omega(\hat{x})d\omega + \int_0^1\int_0^{\omega_m}\tilde{Q}_\omega(x')\frac{G_\omega(\hat{x},\hat{x}')}{\mathrm{Kn}_\omega}d\omega d\hat{x}'\right], \tag{A8}$$

and the kernel function becomes

$$K(\hat{x},\hat{x}') = \frac{1}{2\int_0^{\omega_m}\frac{C_\omega}{\tau_\omega}d\omega}\int_0^{\omega_m}\frac{C_\omega G_\omega(\hat{x},\hat{x}')}{\mathrm{Kn}_\omega\tau_\omega}d\omega. \tag{A9}$$

With these results, the problem can be solved by following the same procedures described in Sec. II B are followed to formulate a linear system of equations. The solution of this system then yields the temperature Fourier coefficients.

APPENDIX B: FOURIER COEFFICIENTS FOR NONBLACK DIFFUSE BOUNDARIES

In this section, we derive the expansion coefficients for a thin film with nonblack, diffuse boundaries. For steady-state heat conduction between two non-black walls as studied in Sec. III, the inhomogeneous function becomes

$$f(\hat{x}) = \frac{1}{2\int_0^{\omega_m}\frac{C_\omega}{\tau_\omega}d\omega}\int_0^{\omega_m}\frac{C_\omega}{\tau_\omega}\left[A_{1\omega}E_2\left(\frac{\hat{x}}{\mathrm{Kn}_\omega}\right) + A_{2\omega}E_2\left(\frac{1-\hat{x}}{\mathrm{Kn}_\omega}\right)\right]d\omega. \tag{B1}$$

Its Fourier coefficients in Eq. (17) are then given by

$$f_0 = \frac{1}{2\int_0^{\omega_m}\frac{C_\omega}{\tau_\omega}d\omega}\int_0^{\omega_m}\frac{C_\omega\mathrm{Kn}_\omega}{\tau_\omega}(A_{1\omega}+A_{2\omega})\left[1-2E_3\left(\frac{1}{\mathrm{Kn}_\omega}\right)\right]d\omega, \tag{B2}$$

and

$$f_n = \frac{1}{\int_0^{\omega_m}\frac{C_\omega}{\tau_\omega}d\omega}\int_0^{\omega_m}\int_0^1\frac{C_\omega}{\tau_\omega}\mathrm{Kn}_\omega\mu\frac{\left[A_{1\omega}+(-1)^nA_{2\omega}\right]-e^{-\frac{1}{\mathrm{Kn}_\omega\mu}}\left[(-1)^nA_{1\omega}+A_{2\omega}\right]}{1+(\mathrm{Kn}_\omega\mu)^2(n\pi)^2}, \tag{B3}$$

providing the right-hand side of Eq. (22). Under the same assumption of diffuse, non-black walls, the kernel function becomes

$$K(\hat{x},\hat{x}') = \frac{1}{2\int_0^{\omega_m}\frac{C_\omega}{\tau_\omega}d\omega}\int_0^{\omega_m}\frac{C_\omega G_\omega(\hat{x},\hat{x}')}{\mathrm{Kn}_\omega\tau_\omega}d\omega, \tag{B4}$$

where

$$G_\omega(\hat{x},\hat{x}') = E_2\left(\frac{\hat{x}}{\mathrm{Kn}_\omega}\right)\left[D_\omega E_1\left(\frac{1-\hat{x}'}{\mathrm{Kn}_\omega}\right) + B_{1\omega}E_1\left(\frac{\hat{x}'}{\mathrm{Kn}_\omega}\right)\right] + E_2\left(\frac{1-\hat{x}}{\mathrm{Kn}_\omega}\right)\left[D_\omega E_1\left(\frac{\hat{x}'}{\mathrm{Kn}_\omega}\right) + B_{1\omega}E_1\left(\frac{1-\hat{x}'}{\mathrm{Kn}_\omega}\right)\right] + E_1\left(\frac{|\hat{x}-\hat{x}'|}{\mathrm{Kn}_\omega}\right). \tag{B5}$$

Its Fourier coefficients k_{mn} are given by Eq. (18), and can be evaluated as

$$k_{00} = \frac{2}{\int_0^{\omega_m}\frac{C_\omega}{\tau_\omega}d\omega}\int_0^{\omega_m}\frac{C_\omega \mathrm{Kn}_\omega}{\tau_\omega}\left\{\frac{2}{\mathrm{Kn}_\omega} - 1 + 2E_3\left(\frac{1}{\mathrm{Kn}_\omega}\right) + (2D_\omega + B_{1\omega} + B_{2\omega})\right.$$
$$\left.\times\left[\frac{1}{2} - E_3\left(\frac{1}{\mathrm{Kn}_\omega}\right) - \frac{1}{2}E_2\left(\frac{1}{\mathrm{Kn}_\omega}\right) + E_3\left(\frac{1}{\mathrm{Kn}_\omega}\right)E_2\left(\frac{1}{\mathrm{Kn}_\omega}\right)\right]\right\}d\omega, \tag{B6}$$

and

$$k_{m0} = \frac{2}{\int_0^{\omega_m}\frac{C_\omega}{\tau_\omega}d\omega}\int_0^{\omega_m}\frac{C_\omega}{\tau_\omega}\int_0^1\frac{\mathrm{Kn}_\omega\mu\left[(-1)^m+1\right]\left[e^{-\frac{1}{\mathrm{Kn}_\omega\mu}}-1\right]}{1+(\mathrm{Kn}_\omega\mu)^2(m\pi)^2}d\mu d\omega + \frac{2}{\int_0^{\omega_m}\frac{C_\omega}{\tau_\omega}d\omega}\int_0^{\omega_m}\frac{C_\omega}{\tau_\omega}(D_\omega+B_{1\omega})\left[1-E_2\left(\frac{1}{\mathrm{Kn}_\omega}\right)\right]$$
$$\times\int_0^1\frac{\mathrm{Kn}_\omega\mu\left[1-(-1)^m e^{-\frac{1}{\mathrm{Kn}_\omega\mu}}\right]}{1+(\mathrm{Kn}_\omega\mu)^2(m\pi)^2}d\mu d\omega + \frac{2}{\int_0^{\omega_m}\frac{C_\omega}{\tau_\omega}d\omega}\int_0^{\omega_m}\frac{C_\omega}{\tau_\omega}(D_\omega+B_{2\omega})\left[1-E_2\left(\frac{1}{\mathrm{Kn}_\omega}\right)\right]\int_0^1\frac{\mathrm{Kn}_\omega\mu\left[(-1)^m-e^{-\frac{1}{\mathrm{Kn}_\omega\mu}}\right]}{1+(\mathrm{Kn}_\omega\mu)^2(m\pi)^2}d\mu d\omega, \tag{B7}$$

and

$$k_{0n} = \frac{2}{\int_0^{\omega_m}\frac{C_\omega}{\tau_\omega}d\omega}\int_0^{\omega_m}\frac{C_\omega}{\tau_\omega}\int_0^1\frac{\mathrm{Kn}_\omega\mu\left[(-1)^n+1\right]\left[e^{-\frac{1}{\mathrm{Kn}_\omega\mu}}-1\right]}{1+(\mathrm{Kn}_\omega\mu)^2(n\pi)^2}d\mu d\omega + \frac{2}{\int_0^{\omega_m}\frac{C_\omega}{\tau_\omega}d\omega}\int_0^{\omega_m}\frac{C_\omega \mathrm{Kn}_\omega}{\tau_\omega}(D_\omega+B_{1\omega})\left[\frac{1}{2}-E_3\left(\frac{1}{\mathrm{Kn}_\omega}\right)\right]$$
$$\times\int_0^1\frac{\left[1-(-1)^n e^{-\frac{1}{\mathrm{Kn}_\omega\mu}}\right]}{1+(\mathrm{Kn}_\omega\mu)^2(n\pi)^2}d\mu d\omega + \frac{2}{\int_0^{\omega_m}\frac{C_\omega}{\tau_\omega}d\omega}\int_0^{\omega_m}\frac{C_\omega \mathrm{Kn}_\omega}{\tau_\omega}(D_\omega+B_{2\omega})\left[\frac{1}{2}-E_3\left(\frac{1}{\mathrm{Kn}_\omega}\right)\right]\int_0^1\frac{\left[(-1)^n-e^{-\frac{1}{\mathrm{Kn}_\omega\mu}}\right]}{1+(\mathrm{Kn}_\omega\mu)^2(n\pi)^2}d\mu d\omega, \tag{B8}$$

and for $m \neq n$

$$k_{mn} = \frac{2}{\int_0^{\omega_m}\frac{C_\omega}{\tau_\omega}d\omega}\int_0^{\omega_m}\frac{C_\omega}{\tau_\omega}\int_0^1\frac{\mathrm{Kn}_\omega\mu\left\{e^{-\frac{1}{\mathrm{Kn}_\omega\mu}}\left[(-1)^m+(-1)^n\right]-\left[1+(-1)^{m+n}\right]\right\}}{\left[1+(\mathrm{Kn}_\omega\mu)^2(m\pi)^2\right]\left[1+(\mathrm{Kn}_\omega\mu)^2(n\pi)^2\right]}d\mu d\omega$$
$$+\frac{2}{\int_0^{\omega_m}\frac{C_\omega}{\tau_\omega}d\omega}\int_0^{\omega_m}\frac{C_\omega D_\omega}{\tau_\omega}\int_0^1\frac{\mathrm{Kn}_\omega\mu\left[1-(-1)^m e^{-\frac{1}{\mathrm{Kn}_\omega\mu}}\right]}{1+(\mathrm{Kn}_\omega\mu)^2(m\pi)^2}d\mu\int_0^1\frac{\left[(-1)^n-e^{-\frac{1}{\mathrm{Kn}_\omega\mu}}\right]}{1+(\mathrm{Kn}_\omega\mu)^2(n\pi)^2}d\mu d\omega$$
$$+\frac{2}{\int_0^{\omega_m}\frac{C_\omega}{\tau_\omega}d\omega}\int_0^{\omega_m}\frac{C_\omega D_\omega}{\tau_\omega}\int_0^1\frac{\mathrm{Kn}_\omega\mu\left[(-1)^m-e^{-\frac{1}{\mathrm{Kn}_\omega\mu}}\right]}{1+(\mathrm{Kn}_\omega\mu)^2(m\pi)^2}d\mu\int_0^1\frac{\left[1-(-1)^n e^{-\frac{1}{\mathrm{Kn}_\omega\mu}}\right]}{1+(\mathrm{Kn}_\omega\mu)^2(n\pi)^2}d\mu d\omega$$
$$+\frac{2}{\int_0^{\omega_m}\frac{C_\omega}{\tau_\omega}d\omega}\int_0^{\omega_m}\frac{C_\omega B_{1\omega}}{\tau_\omega}\int_0^1\frac{\mathrm{Kn}_\omega\mu\left[1-(-1)^m e^{-\frac{1}{\mathrm{Kn}_\omega\mu}}\right]}{1+(\mathrm{Kn}_\omega\mu)^2(m\pi)^2}d\mu\int_0^1\frac{\left[1-(-1)^n e^{-\frac{1}{\mathrm{Kn}_\omega\mu}}\right]}{1+(\mathrm{Kn}_\omega\mu)^2(n\pi)^2}d\mu d\omega$$
$$+\frac{2}{\int_0^{\omega_m}\frac{C_\omega}{\tau_\omega}d\omega}\int_0^{\omega_m}\frac{C_\omega B_{2\omega}}{\tau_\omega}\int_0^1\frac{\mathrm{Kn}_\omega\mu\left[(-1)^m-e^{-\frac{1}{\mathrm{Kn}_\omega\mu}}\right]}{1+(\mathrm{Kn}_\omega\mu)^2(m\pi)^2}d\mu\int_0^1\frac{\left[(-1)^n-e^{-\frac{1}{\mathrm{Kn}_\omega\mu}}\right]}{1+(\mathrm{Kn}_\omega\mu)^2(n\pi)^2}d\mu d\omega, \tag{B9}$$

and for $m \neq 0$

$$k_{mm} = \frac{2}{\int_0^{\omega_m} \frac{C_\omega}{\tau_\omega} d\omega} \left\{ \int_0^{\omega_m} \frac{C_\omega}{\tau_\omega} \frac{\tan^{-1}(m\pi \mathrm{Kn}_\omega)}{m\pi \mathrm{Kn}_\omega} d\omega + 2 \int_0^{\omega_m} \frac{C_\omega}{\tau_\omega} \int_0^1 \frac{\mathrm{Kn}_\omega \mu \left[e^{-\frac{1}{(-1)^m \mathrm{Kn}_\omega \mu}} - 1 \right]}{\left[1 + (\mathrm{Kn}_\omega \mu)^2 (m\pi)^2 \right]^2} d\mu d\omega \right\}$$
$$+ \frac{2}{\int_0^{\omega_m} \frac{C_\omega}{\tau_\omega} d\omega} \int_0^{\omega_m} \frac{C_\omega D_\omega}{\tau_\omega} \int_0^1 \frac{\mathrm{Kn}_\omega \mu \left[1 - (-1)^m e^{-\frac{1}{\mathrm{Kn}_\omega \mu}} \right]}{1 + (\mathrm{Kn}_\omega \mu)^2 (m\pi)^2} d\mu \int_0^1 \frac{\left[(-1)^m - e^{-\frac{1}{\mathrm{Kn}_\omega \mu}} \right]}{1 + (\mathrm{Kn}_\omega \mu)^2 (m\pi)^2} d\mu d\omega$$
$$+ \frac{2}{\int_0^{\omega_m} \frac{C_\omega}{\tau_\omega} d\omega} \int_0^{\omega_m} \frac{C_\omega D_\omega}{\tau_\omega} \int_0^1 \frac{\mathrm{Kn}_\omega \mu \left[(-1)^m - e^{-\frac{1}{\mathrm{Kn}_\omega \mu}} \right]}{1 + (\mathrm{Kn}_\omega \mu)^2 (m\pi)^2} d\mu \int_0^1 \frac{\left[1 - (-1)^m e^{-\frac{1}{\mathrm{Kn}_\omega \mu}} \right]}{1 + (\mathrm{Kn}_\omega \mu)^2 (m\pi)^2} d\mu d\omega$$
$$+ \frac{2}{\int_0^{\omega_m} \frac{C_\omega}{\tau_\omega} d\omega} \int_0^{\omega_m} \frac{C_\omega B_{1\omega}}{\tau_\omega} \int_0^1 \frac{\mathrm{Kn}_\omega \mu \left[1 - (-1)^m e^{-\frac{1}{\mathrm{Kn}_\omega \mu}} \right]}{1 + (\mathrm{Kn}_\omega \mu)^2 (m\pi)^2} d\mu \int_0^1 \frac{\left[1 - (-1)^m e^{-\frac{1}{\mathrm{Kn}_\omega \mu}} \right]}{1 + (\mathrm{Kn}_\omega \mu)^2 (m\pi)^2} d\mu d\omega$$
$$+ \frac{2}{\int_0^{\omega_m} \frac{C_\omega}{\tau_\omega} d\omega} \int_0^{\omega_m} \frac{C_\omega B_{2\omega}}{\tau_\omega} \int_0^1 \frac{\mathrm{Kn}_\omega \mu \left[(-1)^m - e^{-\frac{1}{\mathrm{Kn}_\omega \mu}} \right]}{1 + (\mathrm{Kn}_\omega \mu)^2 (m\pi)^2} d\mu \int_0^1 \frac{\left[(-1)^m - e^{-\frac{1}{\mathrm{Kn}_\omega \mu}} \right]}{1 + (\mathrm{Kn}_\omega \mu)^2 (m\pi)^2} d\mu d\omega. \quad \text{(B10)}$$

These equations specify the matrix elements of $\bar{\bar{A}}$ in Eq. (22). With the linear system specified, the coefficients of the temperature profile x_m can be easily obtained by solving a linear system.

[1] D. G. Cahill, P. V. Braun, G. Chen, D. R. Clarke, S. Fan, K. E. Goodson, P. Keblinski, W. P. King, G. D. Mahan, A. Majumdar, H. J. Maris, S. R. Phillpot, E. Pop, and L. Shi, "Nanoscale thermal transport. II. 2003–2012," Appl. Phys. Rev. **1**(1), 011305 (2014).
[2] Y. Wang, H. Huang, and X. Ruan, "Decomposition of coherent and incoherent phonon conduction in superlattices and random multilayers," Phys. Rev. B **90**, 165406 (2014).
[3] X. Wang and B. Huang, "Computational study of in-plane phonon transport in si thin films," Sci. Rep. **4**, 6399 (2014).
[4] A. A. Balandin and D. L. Nika, "Phononics in low-dimensional materials," Mater. Today **15**(6), 266–275 (2012).
[5] I. Chowdhury, R. Prasher, K. Lofgreen, G. Chrysler, S. Narasimhan, R. Mahajan, D. Koester, R. Alley, and R. Venkatasubramanian, "On-chip cooling by superlattice-based thin-film thermoelectrics," Nat. Nanotechnol. **4**(4), 235–238 (2009).
[6] Z. Su, L. Huang, F. Liu, J. P. Freedman, L. M. Porter, R. F. Davis, and J. A. Malen, "Layer-by-layer thermal conductivities of the Group III nitride films in blue/green light emitting diodes," Appl. Phys. Lett. **100**(20), 201106 (2012).
[7] A. L. Moore and L. Shi, "Emerging challenges and materials for thermal management of electronics," Mater. Today **17**(4), 163–174 (2014).
[8] Z. Yan, G. Liu, J. M. Khan, and A. A. Balandin, "Graphene quilts for thermal management of high power gan transistors," Nat. Commun. **3**, 827 (2012).
[9] Y. K. Koh, Y. Cao, F. Liu, D. G. Cahill, and D. Jena, "Heat-transport mechanisms in superlattices," Adv. Functional Mater. **19**(4), 610–615 (2009).
[10] J. Cho, Y. Li, W. E. Hoke, D. H. Altman, M. Asheghi, and K. E. Goodson, "Phonon scattering in strained transition layers for gan heteroepitaxy," Phys. Rev. B **89**, 115301 (2014).
[11] F. Fuchs, "The conductivity of thin metallic films according to the electron theory of metals," Proc. Cambridge Philos. Soc. **34**, 100–108 (1938).
[12] E. H. Sondheimer, "The mean free path of electrons in metals," Adv. Phys. **1**, 1–42 (1952).
[13] G. Chen and C. L. Tien, "Thermal conductivities of quantum well structures," J. Thermophys. Heat Transfer **7**, 311–318 (1993).
[14] G. Chen, "Size and interface effects on thermal conductivity of superlattices and periodic thin-film structures," J. Heat Transfer **119**, 220–229 (1997).
[15] S. Mazumder and A. Majumdar, "Monte Carlo study of phonon transport in solid thin films including dispersion and polarization," J. Heat Transfer **123**, 749–759 (2001).
[16] S. Chandrasekhar and G. Münch, "The Theory of the Fluctuations in Brightness of the Milky way I," Astrophys. J. **112**, 380 (1950).
[17] R. Bellman and G. M. Wing, *An Introduction to Invariant Imbedding* (Wiley, New York, 1975).
[18] K. M. Case and P. F. Zweifel, *Linear Transport Theory* (Addison-Wesley Publishing Company, Inc, 1967).
[19] C. C. Lii and M. N. Ziik, "Transient radiation and conduction in an absorbing, emitting, scattering slab with reflective boundaries," Int. J. Heat Mass Transfer **15**(5), 1175–1179 (1972).
[20] A. Majumdar, "Microscale heat conduction in dielectric thin films," J. Heat Transfer **115**, 7–16 (1993).
[21] A. A. Joshi and A. Majumdar, "Transient ballistic and diffusive phonon heat transport in thin films," J. Appl. Phys. **74**(1), 31–39 (1993).
[22] G. Chen, "Thermal conductivity and ballistic-phonon transport in the cross-plane direction of superlattices," Phys. Rev. B **57**, 14958–14973 (1998).
[23] G. Chen and T. F. Zeng, "Nonequilibrium phonon and electron transport in heterostructures and superlattices," Microscale Thermophys. Eng. **5**, 71–88 (2001).
[24] T. F. Zeng and G. Chen, "Phonon heat conduction in thin films: Impact of thermal boundary resistance and internal heat generation," J. Heat Transfer **123**, 340–347 (2001).
[25] K. Esfarjani, G. Chen, and H. T. Stokes, "Heat transport in silicon from first-principles calculations," Phys. Rev. B **84**(8), 085204 (2011).
[26] A. Ward and D. A. Broido, "Intrinsic phonon relaxation times from first-principles studies of the thermal conductivities of si and ge," Phys. Rev. B **81**, 085205 (2010).
[27] A. D. Polyanin and A. V. Manzhirov, *Handbook of Integral Equations* (Chapman & Hall/CRC, 2008).
[28] G. Chen, *Nanoscale Energy Transport and Conversion* (Oxford University Press, New York, 2005).
[29] H. F. Weinberger, *A First Course in Partial Differential Equations with Complex Variables and Transform Methods* (Dover Publications, Inc., 1995).
[30] A. J. Minnich, G. Chen, S. Mansoor, and B. S. Yilbas, "Quasiballistic heat transfer studied using the frequency-dependent Boltzmann transport equation," Phys. Rev. B **84**, 235207 (2011).

[31]A. J. Minnich, "Determining phonon mean free paths from observations of quasiballistic thermal transport," Phys. Rev. Lett. **109**, 205901 (2012).
[32]T.-K. Hsiao, H.-K. Chang, S.-C. Liou, M.-W. Chu, S.-C. Lee, and C.-W. Chang, "Observation of room-temperature ballistic thermal conduction persisting over 8.3 μm in sige nanowires," Nat. Nanotechnol. **8**, 534–538 (2013).
[33]X. Xu, L. F. C. Pereira, Y. Wang, J. Wu, K. Zhang, X. Zhao, S. Bae, C. T. Bui, R. Xie, J. T. T. L. Thong, B. H. Hong, K. P. Loh, D. Donadio, B. Li, and B. Ozyilmaz, "Length-dependent thermal conductivity in suspended single-layer graphene," Nat. Commun. **5**, 3689 (2014).
[34]H. Zhang, C. Hua, D. Ding, and A. Minnich, "Length dependent thermal conductivity measurements yield phonon mean free path spectra in nanostructures," Sci. Rep. **5**, 9121 (2015).